Electronic Supplementary Information

Label-free OIRD microarray chips with nanostructured sensing interface: enhanced sensitivity and mechanism

Xiaoyi Li, [a] Changxiang Fang, [a] Zhihao Feng, [a] Junying Li, [a] Yan Li [b] and Weihua Hu*[a]

[a] Key Laboratory of Luminescent and Real-Time Analytical Chemistry (Southwest University), Ministry of Education, School of Materials and Energy, Southwest University, Chongqing 400715, China

[b] Analytical & Testing Center, Southwest University Chongqing 400715, China.

* Corresponding author Email: whhu@swu.edu.cn (W. H. Hu)

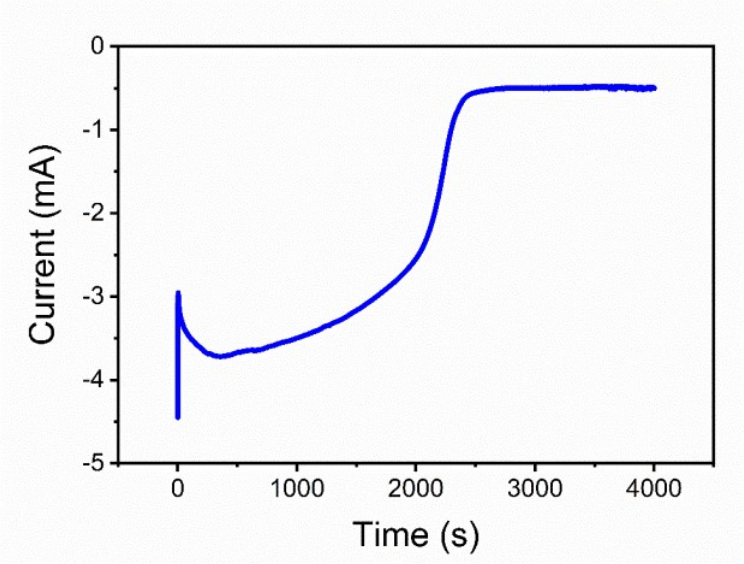

Fig. S1. Representative chronoamperometric curve of FTO etching at -0.8 V vs. Ag/AgCl in acid.

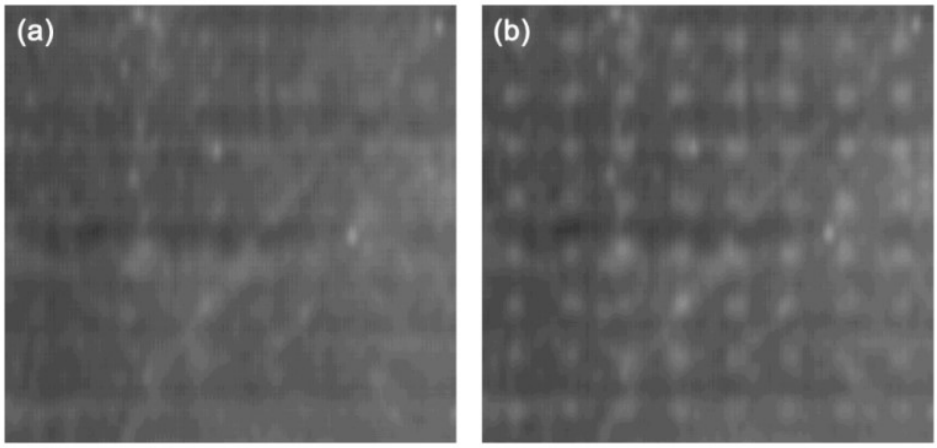

Fig. S2. OIRD images of etched FTO-based microarray before (a) and after (b) reacting with 10 μg mL^{-1} streptavidin.

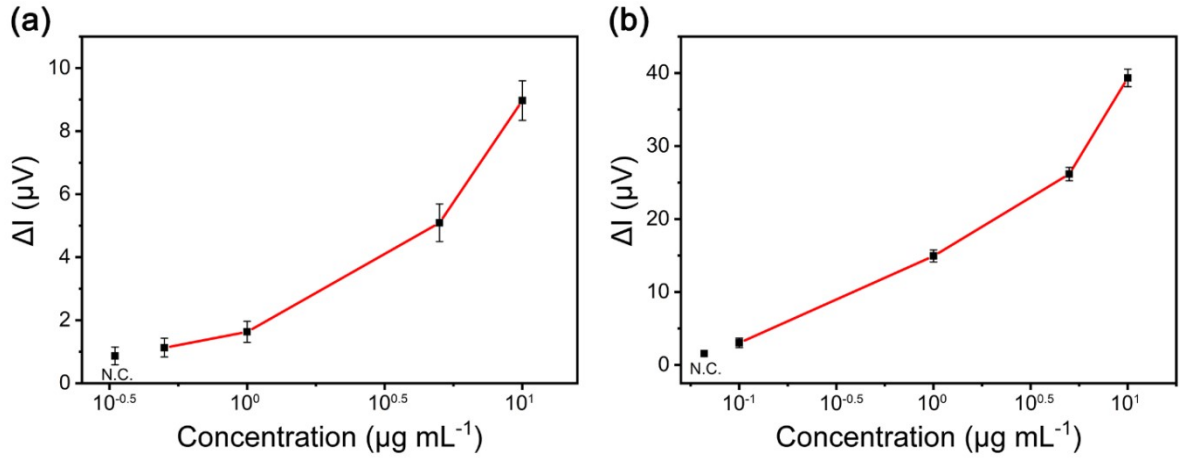

Fig. S3. Dose-response curve for detection of streptavidin on glass-based (a) and pristine FTO (b) based microarrays.

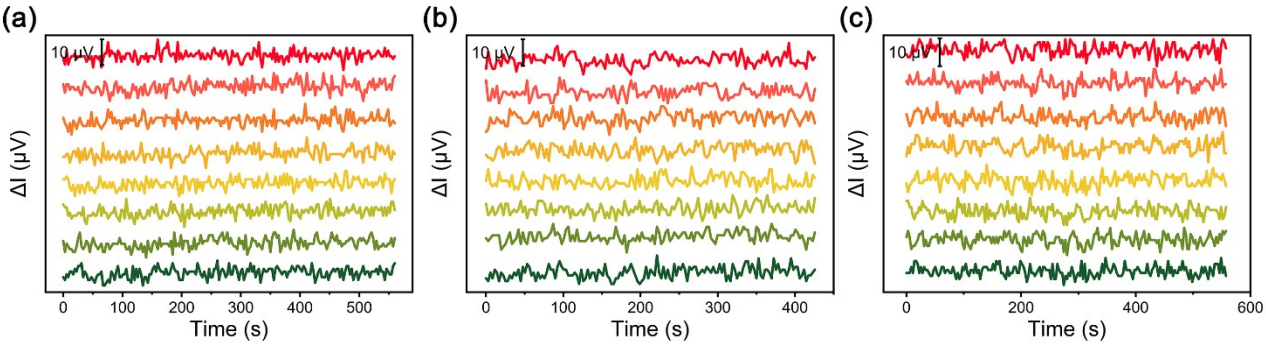

Fig. S4. *In situ* OIRD signals collected on glass (a), pristine FTO (b) and etched FTO (c) based microarrays in 0.01 M PBS buffer. For each chip, the signals collected on 8 spots were shown.

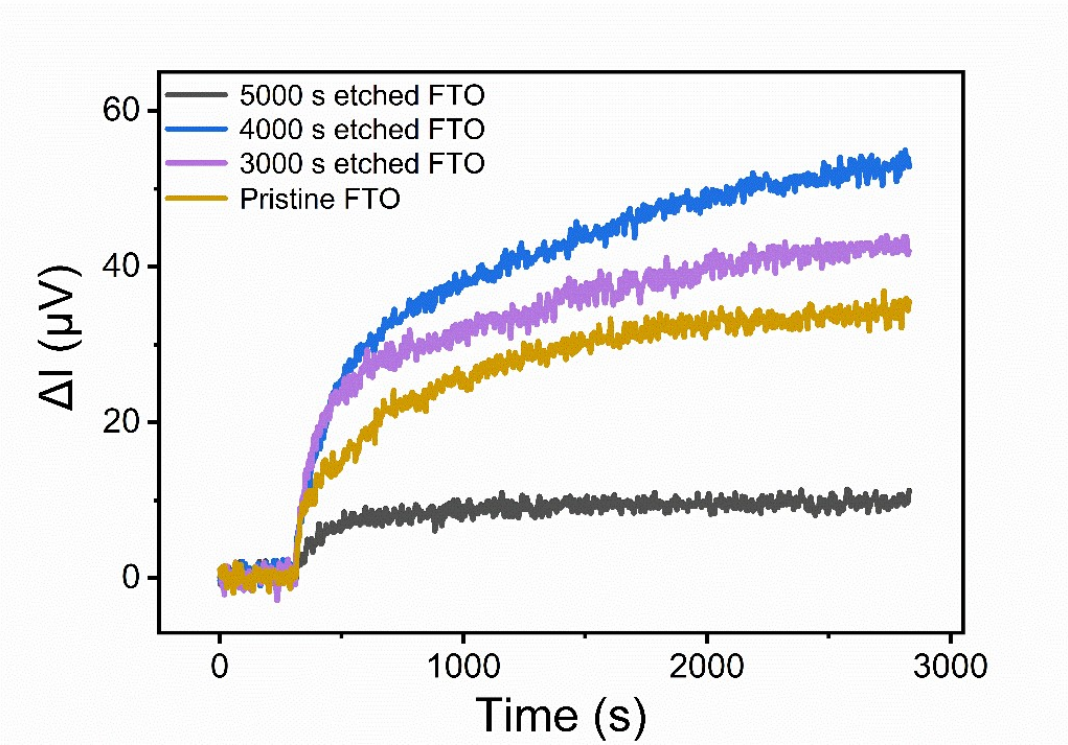

Fig. S5. *In situ* OIRD signals for detection of 10 μg mL^{-1} streptavidin on etched FTO based chips with different etching times.

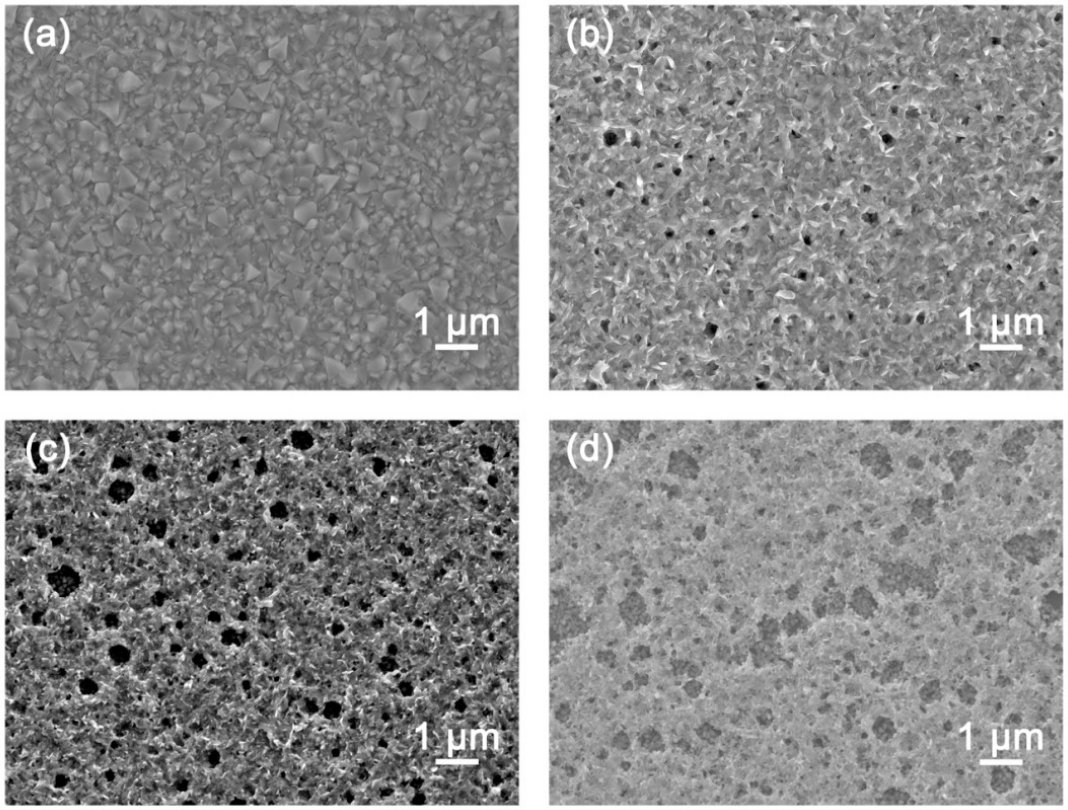

Fig. S6. SEM images of pristine FTO (a), etched FTO for 3000 s (b), 4000 s (c) and 5000 s (d) etching.

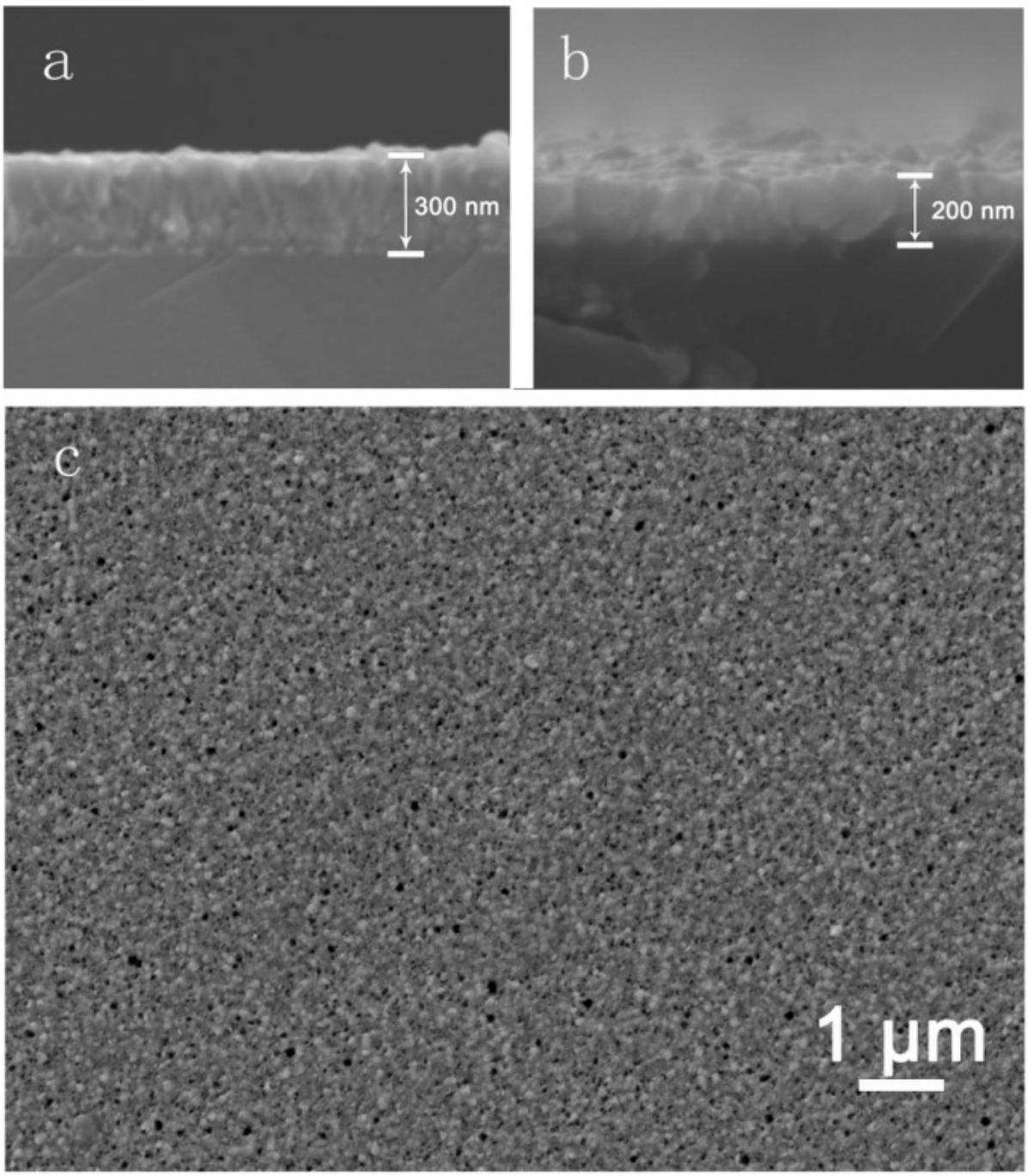

Fig. S7. Section SEM image of 300 nm FTO (a), 200 nm FTO (b), and surface image of 200 nm FTO (c). We note that 200 nm FTO was obtained by electrochemically etching of 300 nm FTO at -0.8 V in O_2 saturated 0.5 M H_2SO_4 for 1000 s. We did so because 300 nm FTO is the thinnest one commercially available to us; we do not find 200 nm FTO in the market. From (b, c) it is found that after 1000 s etching of 300 nm FTO, the FTO thickness was decreased to 200 nm and no rich or pronounced nanostructures were formed on its surface, which is sharply different with 4000 s etched FTO from 800 nm FTO, as shown in Fig 2(c, d). Therefore we use this slightly etched FTO as a smooth 200 nm FTO for comparison.

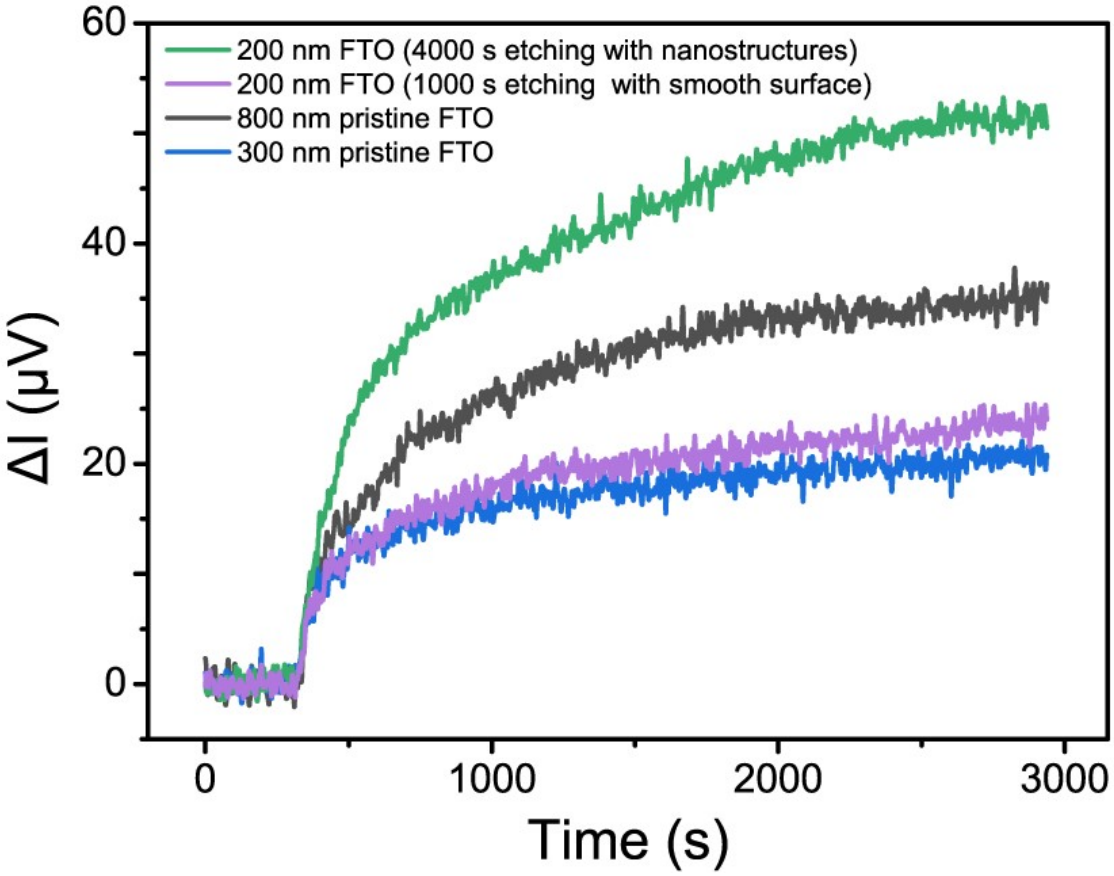

Fig. S8. OIRD *in situ* responses towards streptavidin target at 10 ng mL^{-1} spiked in 10% serum obtained on various chips. It is found that the 200 nm FTO based chip obtained by 4000 s etching 800 nm FTO shows highest signal. Particularly it is higher than that based on 200 nm FTO obtained by 1000 s etching 300 nm FTO. If considering the same FTO thickness of 200 nm, the significantly enhanced response could be assigned to the nanostructured sensing interface of the 4000 s etched FTO-based chip. The higher response on 800 nm FTO than 300 nm FTO implies the profound influence of FTO thickness as we previously revealed.

Kinetics fitting

For biomolecular affinity binding between immobilized probe and target in solution, the kinetics follows the first-order kinetics at the initial stage when the captured target on the surface is low and the diffusion transport of target should be considered for the whole reaction. The kinetics is given by:

$$\Gamma_{Ab}(\bar{t}) = c_0\sqrt{D\tau}[2\sqrt{\frac{\bar{t}}{\pi}} + \exp(\bar{t})erfc(\sqrt{\bar{t}}) - 1] \quad \text{(E1)}$$

Among them, Γ_{Ab} is the surface concentration of the captured target and is proportional to OIRD signal in our work. c_0 is the bulk concentration of the target. $erfc$ is the complementary error function. D is the diffusion coefficient of the target. $\bar{t} = \frac{t}{\tau}$, and $\tau = \frac{D}{k_1^2 \Gamma_0^2}$, where k_1 is the forward association rate constant of the bio-affinity reaction; Γ_0 is the surface concentration of attached probes on the surface at beginning. The fitting shown in Figure 2a is achieved using (E1).

Optical computation

OIRD achieves real time monitoring of surface/interface processes by measuring the time-lapsed difference between the relative changes in the reflectivity of p-polarized light and s-polarized light. Δ_p and Δ_s represent the relative changes of p-polarized light reflectance and s-polarized light reflectance, respectively and are defined as:

$$\Delta_p = \frac{r_p - r_{p0}}{r_{p0}} \qquad \text{(E2)}$$

$$\Delta_s = \frac{r_s - r_{s0}}{r_{s0}} \qquad \text{(E3)}$$

Where r_{p0} and r_{s0} are the initial p- and s-polarized reflectivity of the interface, and r_p and r_s are the final p- and s-polarized reflectivity of the interface. Defining OIRD signal as $\Delta_p - \Delta_s$, then:

$$\Delta_p - \Delta_s = \frac{r_p - r_{p0}}{r_{p0}} - \frac{r_s - r_{s0}}{r_{s0}} = \frac{\delta r_p}{r_{p0}} - \frac{\delta r_s}{r_{s0}} \qquad \text{(E4)}$$

According to the optical transmission matrix, the normalized OIRD frequency-doubling signal is proportional to the imaginary part of the reflection difference $\Delta_p - \Delta_s$, namely:

$$R_e\{\Delta p - \Delta s\} \approx \frac{1}{2J_2 A}\left(\frac{I(2\Omega)}{I_{DC}}\right) \qquad \text{(E5)}$$

This signal directly reflects the change in reflectivity from the surface.

The reflectance r_{2p} and r_{2s} can be calculated directly by Fresnel formula when only the detection environment and the glass slide constitute a two-layer system(Figure 7a):

$$r_{2p} = \frac{\sqrt{\varepsilon_0(\varepsilon_s - \varepsilon_0 sin^2\varphi_{inc})} - \varepsilon_s cos\varphi_{inc}}{\sqrt{\varepsilon_0(\varepsilon_s - \varepsilon_0 sin^2\varphi_{inc})} + \varepsilon_s cos\varphi_{inc}} \quad \text{(E6)}$$

$$r_{2s} = \frac{\sqrt{\varepsilon_0} cos\varphi_{inc} - \sqrt{\varepsilon_s - \varepsilon_0 sin^2\varphi_{inc}}}{\sqrt{\varepsilon_0} cos\varphi_{inc} + \sqrt{\varepsilon_s - \varepsilon_0 sin^2\varphi_{inc}}} \quad \text{(E7)}$$

When the surface is covered with the target, the transmission matrix can be used to calculate the reflectivity r_{3p} and r_{3s} of p-polarized light and s-polarized light respectively.

Transmission matrix of p-polarized light and s-polarized light:

$$M_p = \begin{bmatrix} m_{11} & m_{12} \\ m_{21} & m_{22} \end{bmatrix} = \begin{bmatrix} \cos\delta & \frac{-i\sin\delta}{p_d} \\ -ip_d\sin\delta & \cos\delta \end{bmatrix} \quad \text{(E8)}$$

$$M_s = \begin{bmatrix} m_{11} & m_{12} \\ m_{21} & m_{22} \end{bmatrix} = \begin{bmatrix} \cos\delta & \frac{-i\sin\delta}{q_d} \\ -iq_d\sin\delta & \cos\delta \end{bmatrix} \quad \text{(E9)}$$

$\delta = \frac{2\pi}{\lambda} d\sqrt{\varepsilon_d - \varepsilon_0 sin^2\varphi_{inc}}$ is the phase difference introduced as light propagates through the film layer.

Then r_{3p} and r_{3s} can be written as:

$$r_{3p} = \frac{p_0 m_{11} + p_0 p_s m_{12} - m_{21} - p_s m_{22}}{p_0 m_{11} + p_0 p_s m_{12} + m_{21} + p_s m_{22}} \quad \text{(E10)}$$

$$r_{3s} = \frac{q_0 m_{11} + q_0 q_s m_{12} - m_{21} - q_s m_{22}}{q_0 m_{11} + q_0 q_s m_{12} + m_{21} + q_s m_{22}} \quad \text{(E11)}$$

In this case, $p_0 = \sqrt{\varepsilon_0} cos\varphi_{inc}$, $p_d = \sqrt{\varepsilon_d} cos\varphi_d$, $p_s = \sqrt{\varepsilon_s} cos\varphi_s$, $q_0 = \sqrt{\varepsilon_0} cos\varphi_{inc}$, $q_d = \sqrt{\varepsilon_d} cos\varphi_d$, $q_s = \sqrt{\varepsilon_s} cos\varphi_s$.

When the film thickness is much smaller than the light wavelength ($d \ll \lambda$), OIRD signal ($\Delta_p - \Delta_s$) can be simplified as:

$$\Delta_p - \Delta_s = \frac{(-i)4\pi d\sqrt{\varepsilon_0}\varepsilon_s cos\varphi_{inc} sin^2\varphi_{inc} \quad (\varepsilon_d - \varepsilon_0)(\varepsilon_d - \varepsilon_s)}{\lambda(\varepsilon_s - \varepsilon_0)(\varepsilon_s cos^2\varphi_{inc} - \varepsilon_0 sin^2\varphi_{inc}) \qquad \varepsilon_d} \quad \text{(E12)}$$

The above formula shows that, OIRD signal ($\Delta_p - \Delta_s$) is closely related to ε_0, ε_d, d, ε_s, λ, φ_{inc}. Under the condition that the experimental environment is consistent with the wavelength and incident Angle of the incident laser, the dielectric constant and the thickness of the film layer are the main factors that really affect the change of OIRD signal intensity. The dielectric constant of the target layer could also be treated as constant as all the biomolecules remains the same. When $d \ll \lambda$ (wavelength of the laser, 632.8 nm), $\Delta I(2\Omega)$ is proportional to d, which sets the base for quantitative detection with OIRD.

For detection on FTO-based chip, the interface architecture is changed from glass/FTO/solution three-layer model to glass/FTO/target/solution four-layer model (Figure 7b). Before detection, the chip can be viewed as a glass/FTO/solution three-layer model (Figure 7b), where FTO layer includes FTO layer and attached probes. ε_s, ε_p and ε_0 represent the dielectric constants of glass, FTO and solution, respectively. φ_s, φ_p and φ_0 represent the angles of incidence in glass, FTO and solution. h represents the thickness of FTO layer.

The OIRD signal ($I(2\Omega)$) collected on the surface of the microarray chip is described as:

$$I(2\Omega) = I_0(|r_{3p}|^2\cos^2\alpha - |r_{3s}|^2\sin^2\alpha)J_2(A) \qquad \text{(E13)}$$

Among them, r_{3p} and r_{3s} represent the reflectance of p-polarized light and s-polarized light at the FTO/solution interface, respectively. $|r_{3p}|$ and $|r_{3s}|$ are the amplitudes of r_{3p} and r_{3s}.

After detection, the captured target protein is attached to the chip surface, making the chip form a four-layer model, including glass, FTO, target and solution (Figure 7b). d represents the thickness of the captured target protein. ε_d and φ_d represent the dielectric constant and incident angle of the target protein, respectively.

Similarly, the OIRD signal ($I(2\Omega)$) collected on the surface of the microarray chip can be described as:

$$I(2\Omega) = I_0(|r_{4p}|^2\cos^2\alpha - |r_{4s}|^2\sin^2\alpha)J_2(A) \qquad \text{(E14)}$$

Among them, r_{4p} and r_{4s} represent the reflectance of p-polarized light and s-polarized light at the target/solution interface, respectively. $|r_{4p}|$ and $|r_{4s}|$ are the amplitudes of r_{4p} and r_{4s}.

By subtracting E13 from E14, the OIRD signal ($\Delta I(2\Omega)$) caused by the capture of the target protein can be described as:

$$\Delta I(2\Omega) = I_0[\left(|r_{4p}|^2 - |r_{3p}|^2\right)\cos^2\alpha - \left(|r_{4s}|^2 - |r_{3s}|^2\right)\sin^2\alpha]J_2(A) \quad \text{(E15)}$$

According to the Fresnel formula, the reflectivity of p-polarized light and s-polarized light in the glass/FTO/solution three-layer model respectively are:

$$r_{3p} = \frac{r_{sp}^{(p)} + r_{p0}^{(p)} e^{2i\psi_1}}{1 + r_{sp}^{(p)} r_{p0}^{(p)} e^{2i\psi_1}} \quad \text{(E16)}$$

$$r_{3s} = \frac{r_{sp}^{(s)} + r_{p0}^{(s)} e^{2i\psi_1}}{1 + r_{sp}^{(s)} r_{p0}^{(s)} e^{2i\psi_1}} \quad \text{(E17)}$$

Here,

$$\psi_1 = \frac{2\pi}{\lambda} h \sqrt{\varepsilon_p} \cos\varphi_p \quad \text{(E18)}$$

Among them, $r_{sp}^{(p)}$ and $r_{sp}^{(s)}$ represents the reflectance of p-polarized light and s-polarized light at the glass/FTO interface, respectively. $r_{p0}^{(p)}$ and $r_{p0}^{(s)}$ represent the reflectance of p-polarized light and s-polarized light at the FTO/solution interface, respectively.

According to the optical transmission matrix theory, the reflectivity of p-polarized light and s-polarized light in the glass/FTO/target/solution four-layer model respectively are:

$$r_{4p} = \frac{r_{sp}^{(p)} + r_{pd}^{(p)} e^{2i\psi_1} + r_{d0}^{(p)} e^{2i(\psi_1+\psi_2)} + r_{sp}^{(p)} r_{pd}^{(p)} r_{d0}^{(p)} e^{2i\psi_2}}{1 + r_{sp}^{(p)} r_{pd}^{(p)} e^{2i\psi_1} + r_{sp}^{(p)} r_{d0}^{(p)} e^{2i(\psi_1+\psi_2)} + r_{pd}^{(p)} r_{d0}^{(p)} e^{2i\psi_2}} \quad \text{(E19)}$$

$$r_{4s} = \frac{r_{sp}^{(s)} + r_{pd}^{(s)} e^{2i\psi_1} + r_{d0}^{(s)} e^{2i(\psi_1+\psi_2)} + r_{sp}^{(s)} r_{pd}^{(s)} r_{d0}^{(s)} e^{2i\psi_2}}{1 + r_{sp}^{(s)} r_{pd}^{(s)} e^{2i\psi_1} + r_{sp}^{(s)} r_{d0}^{(s)} e^{2i(\psi_1+\psi_2)} + r_{pd}^{(s)} r_{d0}^{(s)} e^{2i\psi_2}} \quad \text{(E20)}$$

Here,

$$\psi_2 = \frac{2\pi}{\lambda} d \sqrt{\varepsilon_d} \cos\varphi_d \quad \text{(E21)}$$

Among them, $r_{pd}^{(p)}$ and $r_{pd}^{(s)}$ represents the reflectance of p-polarized light and s-polarized light at the FTO/target interface, respectively. $r_{d0}^{(p)}$ and $r_{d0}^{(s)}$ represent the reflectance of p-polarized light and s-polarized light at the target/solution interface, respectively.

In general, the reflectivity of p-polarized light and s-polarized light at the a/b interface can be calculated by the following equation:

$$r_{ab}^{(p)} = \frac{\sqrt{\varepsilon_a}\cos\varphi_b - \sqrt{\varepsilon_b}\cos\varphi_a}{\sqrt{\varepsilon_a}\cos\varphi_b + \sqrt{\varepsilon_b}\cos\varphi_a} \quad \text{(E22)}$$

$$r_{ab}^{(s)} = \frac{\sqrt{\varepsilon_a}\cos\varphi_a - \sqrt{\varepsilon_b}\cos\varphi_b}{\sqrt{\varepsilon_a}\cos\varphi_a + \sqrt{\varepsilon_b}\cos\varphi_b} \quad \text{(E23)}$$

Among them, $r_{ab}^{(p)}$ and $r_{ab}^{(s)}$ represent the reflectance of p-polarized light and s-polarized light at the a/b interface of the substance. ε_a and ε_b represent the dielectric constants of substances a and b, respectively. φ_a and φ_b represent the angles of incidence in media a and b, respectively.

Substitute the equation E16-E23 into the equation E15, and ignore the initial light intensity I_0 and give the corresponding parameters, the variation law of the frequency-doubling signal intensity with the thickness of the polymer layer can be calculated.

Some parameters are assigned to facilitate the calculation: the wavelength of the incident laser λ=632.8nm, the refractive index of the glass slide $n_s = 1.50$, the refractive index of the solution $n_0 = 1.33$, the refractive index of FTO layer $n_p = 2.10$, The refractive index of the bound target protein is $n = 1.52$. It can be seen from the calculation results that the frequency-doubling signal changes with the thickness of the polymer layer, because the polymer layer acts as an interference layer here. On this chip, the $\Delta I(2\Omega)$ signal for a given d of the target thickness (i.e., same target concentration) is influenced by the thickness of FTO layer and significantly enhanced via FTO-aroused interference effect between the two reflected lights from the two (upper and bottom) surfaces of FTO layer, resulting in improved sensitivity on pristine FTO-based chip as observed in this work.

For chip inspection based on etched FTO, the interface architecture is changed from a three-layer glass/FTO/solution model to a four-layer model of glass/FTO/target/solution (Figure 7c). The build of the model is almost identical to the pristine FTO. The only difference is that the dielectric constant of the sensing layer of the etched FTO chip is changed after the immunoreaction. From ε_p before the reaction to $\varepsilon_p + \Delta\varepsilon$ after the reaction. This change is due to the unique structure of the three-dimensional sensing layer, so that the immune response occurs in the entire sensing layer, not just on the surface of the sensing layer.

Similarly, the OIRD signal collected on the surface of the microarray immunochip in the pre-reaction glass/FTO/solution three-layer model and the post-reaction glass/FTO/target/solution four-layer model (I(2Ω)) are described as E14 and E15, respectively.

Since the dielectric constant of the sensing layer after the reaction has changed, the changed dielectric constant is described by $\varepsilon_{p'}$, namely:

$$\varepsilon_{p'} = \varepsilon_p + \Delta\varepsilon \qquad \text{(E24)}$$

Then the changed refractive index of the sensing layer is:

$$n_{p'} = \sqrt{\varepsilon_{p'}} = \sqrt{\varepsilon_p + \Delta\varepsilon} \qquad \text{(E25)}$$

Then, the reflectivity of p-polarized light at the interface between glass and FTO and the reflectivity of p-polarized light at the interface between FTO and target are described as:

$$r_{sp'}^{(p)} = \frac{\sqrt{\varepsilon_s}\cos\varphi_{p'} - \sqrt{\varepsilon_{p'}}\cos\varphi_s}{\sqrt{\varepsilon_s}\cos\varphi_{p'} + \sqrt{\varepsilon_{p'}}\cos\varphi_s} \qquad \text{(E26)}$$

$$r_{p'd}^{(p)} = \frac{\sqrt{\varepsilon_{p'}}\cos\varphi_d - \sqrt{\varepsilon_d}\cos\varphi_{p'}}{\sqrt{\varepsilon_{p'}}\cos\varphi_d + \sqrt{\varepsilon_d}\cos\varphi_{p'}} \qquad \text{(E27)}$$

Similarly, the reflectivity of s-polarized light at the interface between glass and FTO and the reflectivity of s-polarized light at the interface between FTO and target are described as:

$$r_{sp'}^{(s)} = \frac{\sqrt{\varepsilon_s}\cos\varphi_s - \sqrt{\varepsilon_{p'}}\cos\varphi_{p'}}{\sqrt{\varepsilon_s}\cos\varphi_s + \sqrt{\varepsilon_{p'}}\cos\varphi_{p'}} \qquad \text{(E28)}$$

$$r_{p'd}^{(s)} = \frac{\sqrt{\varepsilon_{p'}}\cos\varphi_{p'} - \sqrt{\varepsilon_d}\cos\varphi_d}{\sqrt{\varepsilon_{p'}}\cos\varphi_{p'} + \sqrt{\varepsilon_d}\cos\varphi_d} \qquad \text{(E29)}$$

According to the optical transmission matrix theory, the reflectivity of p-polarized light and s-polarized light in the glass/FTO/target/solution four-layer model respectively are:

$$r_{4p} = \frac{r_{sp'}^{(p)} + r_{p'd}^{(p)} e^{2i\psi_1} + r_{d0}^{(p)} e^{2i(\psi_1+\psi_2)} + r_{sp'}^{(p)} r_{p'd}^{(p)} r_{d0}^{(p)} e^{2i\psi_2}}{1 + r_{sp'}^{(p)} r_{p'd}^{(p)} e^{2i\psi_1} + r_{sp'}^{(p)} r_{d0}^{(p)} e^{2i(\psi_1+\psi_2)} + r_{p'd}^{(p)} r_{d0}^{(p)} e^{2i\psi_2}} \qquad \text{(E30)}$$

$$r_{4s} = \frac{r_{sp'}^{(s)} + r_{p'd}^{(s)} e^{2i\psi_1} + r_{d0}^{(s)} e^{2i(\psi_1+\psi_2)} + r_{sp'}^{(s)} r_{p'd}^{(s)} r_{d0}^{(s)} e^{2i\psi_2}}{1 + r_{sp'}^{(s)} r_{p'd}^{(s)} e^{2i\psi_1} + r_{sp'}^{(s)} r_{d0}^{(s)} e^{2i(\psi_1+\psi_2)} + r_{p'd}^{(s)} r_{d0}^{(s)} e^{2i\psi_2}} \quad \text{(E31)}$$

Here,

$$\psi_2 = \frac{2\pi}{\lambda} d\sqrt{\varepsilon_d}\cos\varphi_d \quad \text{(E32)}$$

Substitute the equation E16-E18 and E24-E32 into the equation E15, and ignore the initial light intensity I_0 and give the corresponding parameters, the variation law of the frequency-doubling signal intensity with the thickness of FTO layer and additional change in effective dielectric constant can be calculated. For simplicity, some parameters are assigned to facilitate the calculation: the wavelength of the incident laser λ=632.8 nm, the refractive index of the glass slide $n_s = 1.50$, the refractive index of the solution $n_0 = 1.33$, the refractive index of FTO layer $n_p = 2.10$, The refractive index of the bound target protein is $n = 1.52$.

Under the given parameters mentioned above, this work calculates the OIRD response ($\Delta I(2\Omega)$) for a given immunoassay reaction (assuming a target layer of d=1 nm) at different FTO thickness (h) in the range of 0-950 nm using E15. The relation between h (thickness of FTO in present work) and the OIRD response ($\Delta I(2\Omega)$) was presented in Fig. S9. From the calculation result, it can be seen that the OIRD response varies and is periodically enhanced with the thickness of FTO layer for a given d = 1 nm. The period is about 320 nm. This is so-called interference enhancement effect as the FTO layer acts as an interference layer here. It can also be seen that the FTO with a thickness of 800 nm can obtain a higher signal than the FTO with a thickness of 300 nm m. This is in good agreement with our experimental observations (Fig. S8).

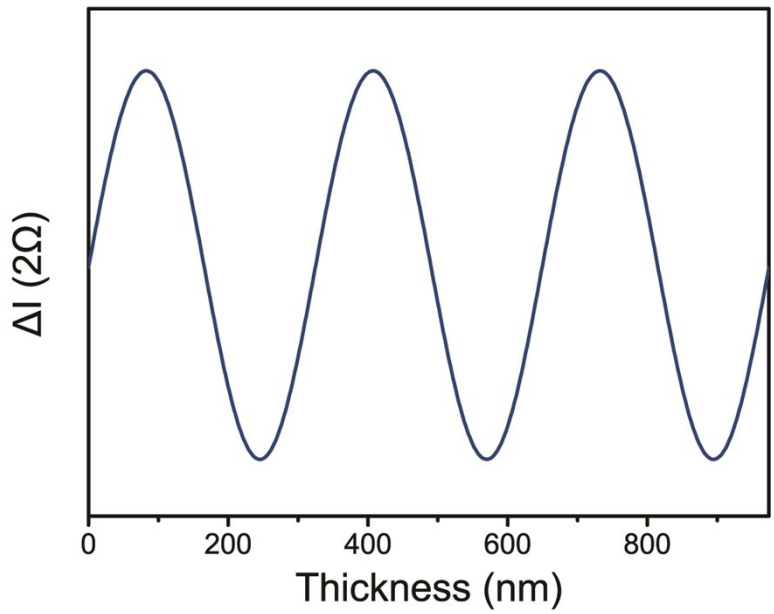

Fig. S9. Calculated interference enhancement of OIRD response. The OIRD signal ($\Delta I(2\Omega)$) toward a same immunoassay reaction of d=1 nm varies and periodically enhanced by the FTO layer in h-dependent manner.

Meanwhile, if the immunoassay reaction on the chip also results in change of dielectric constant of FTO layer ($\Delta\varepsilon_p$), the OIRD response towards this reaction was further enhanced. Assuming a thickness of 200 nm for FTO layer and using E15, we can calculate the relationship between $\Delta\varepsilon_p$ and the OIRD response ($\Delta I(2\Omega)$) when the value of $\Delta\varepsilon_p$ is in the range of 0 to 0.5, as shown in Fig. S8b. From the calculation results, it can be seen that the OIRD response is enhanced in a nearly linear manner with the increase of $\Delta\varepsilon_p$. This is due to the effect of the effective dielectric constant produced by the change in the dielectric constant. For simplicity, the refractive index of nanostructured FTO with probe immobilized was assumed to be 2.10 as well. Meanwhile, the possible complex refractive index was not taken into account in this computation.

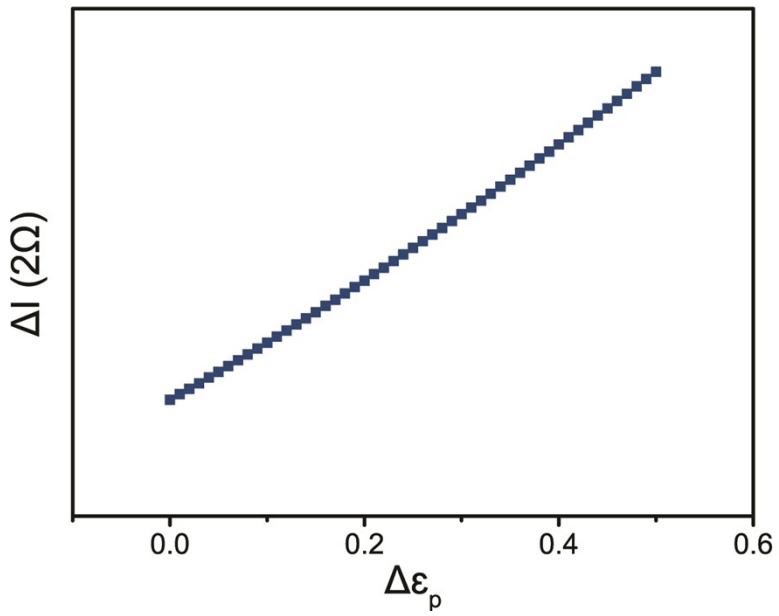

Fig. S9. Relation between OIRD response ($\Delta I(2\Omega)$) and $\Delta\varepsilon_p$ of FTO layer. Assuming a thickness of 1 nm for captured target (d=1 nm). The refractive index and thickness of FTO layer were 2.10 and 200 nm, respectively.

From the calculation results in Fig. S9 and S10, it can be seen that the ΔI(2Ω) signal for a given d of the target thickness (i.e., same target concentration) is influenced by the thickness of FTO layer and change in effective dielectric constant. The nanostructured sensing interface based on FTO layer produces both the interference enhancement effect and the effective dielectric constant effect, thereby improving the detection sensitivity of OIRD.

References including

(1) Liu, S.; Zhu, J. H.; He, L. P.; Dai, J.; Lu, H. B.; Wu, L.; Jin, K. J.; Yang, G. Z.; Zhu, H. *Appl. Phys. Lett.,* **2014,** *104* (16).163701

(2) Zhu, X. D. *Rev. Sci. Instrum.,* **2017,** *88* (8).083112

(3) Zhong, C.; Li, L.; Mei, Y.; Dai, J.; Hu, W.; Lu, Z.; Liu, Y.; Li, C. M.; Lu, H. B. *Sens. Actuators B Chem.,* **2019,** *294*, 216-223

(4) Dai, J., PhD thesis. *Chinese Academy of Sciences and The University of Chinese Academy of Sciences,* **2014**.

(5) Nagib, N. N.; Khodier, S. A. *Opt. Laser. Technol.,* **2000,** *32* (5), 373-377

(6) Born, M.; Wolf, E., Elsevier, **2013**

(7) Zhu, X. D.; Fei, Y. Y.; Wang, X.; Lu, H. B.; Yang, G. Z. *Phys. Rev. B,* **2007,** *75* (24).245434

(8) Miller, J. C.; Zhou, H. P.; Kwekel, J.; Cavallo, R.; Burke, J.; Butler, E. B.; Teh, B. S.; Haab, B. B. *Proteomics,* **2003,** *3* (1), 56-63